Swiss J Geosci (2011) 104:55–66
DOI 10.1007/s00015-010-0047-8

Cement stratigraphy: image probes of cathodoluminescent facies

Aurèle Vuillemin · Mapathe Ndiaye · Rossana Martini · Eric Davaud

Received: 23 February 2010 / Accepted: 25 August 2010 / Published online: 15 February 2011

Abstract Cement stratigraphy of carbonates aims to establish the chronology of processes involved in the rock diagenesis. Regional cement stratigraphy allows correlations and understanding of the petrological heterogeneities in reservoirs and aquifers, but is a long and rigorous approach. This article exposes a methodology of image analysis that facilitates the spatial correlation of diagenetic events in carbonate rocks. Based on the statistical comparison of signals extracted from the red spectrum emission of cathodoluminescence digital images, it gives via crosscorrelation a measure of similarity (values scaled from minimum −1 to maximum 1) between two cathodoluminescence facies. Cementation events and diagenetic chronologies can thus be quickly correlated without the support of a full chronology, the model normally established on cement morphologies, petrological analyses and cathodoluminescence zonation sequences. A case study from two Upper Kimmeridgian Mount Salève outcrops (France) illustrates this methodology. Their diagenetic sequences recorded in cathodoluminescent cements are presented and being compared. The final statistical similarity between the two outcrops reaches an index of $R = 0.78$. This result is sustained by petrological and geochemical analyses such as alizarine–ferricyanure stained thin sections, X microfluorescence mapping of elements, and microthermometry of fluid inclusions.

Editorial Handling: Edwin Gnos and Alan Geoffrey Milnes.

A. Vuillemin (✉) · M. Ndiaye · R. Martini · E. Davaud
Section of Earth and Environmental Sciences,
University of Geneva, 13 rue des Maraîchers,
1205 Geneva, Switzerland
e-mail: aurele.vuillemin@unige.ch

Keywords Cement stratigraphy · Cathodoluminescence · Diagenetic sequence · Image processing · Crosscorrelation

1 Introduction

The signals of cathodoluminescence are used to observe zonations in crystals and permit, in the study of cements, to determine the various steps of diagenesis (Amieux 1982; Richter et al. 2003). The incorporation of luminescence inhibiting and activating elements in carbonate lattices reflects the pore fluids evolution of the system, and gives important information on the diagenetic environment. Luminescence of calcite in sedimentary rocks is activated by the incorporation of manganese in its crystal lattice and inhibited by iron. Fe^{3+} and $Mn^{3/4+}$ have to be reduced to divalent state to substitute calcium. As little as 10–20 ppm Mn^{2+} and 30–35 ppm Fe^{2+} in solid solution are sufficient to produce or quench the luminescence. Although the role of iron still needs further investigation (Cazenave et al. 2003), the Fe^{2+}/Mn^{2+} ratio is supposed to control the intensity of luminescence in carbonate. The reduction of $Mn^{3/4+}$ can take place in sub-oxic waters, reduction of Fe^{3+} in waters of even lower redox potential, sometimes close to anoxia (Plunkett 1997). Calcite luminescence thus often reflects the eH/pH evolution of the interstitial fluids (Machel 1985; Pagel et al. 2000), but many other factors are to be considered, such as: salinity changes, concentrations of metal ions, Ca^{2+} activity, kinetics of crystal growth, sources of organic matter and clay minerals, temporal and spatial variations of pore fluid chemistry, and diagenetic processes (Machel and Burton 1991). These factors also trigger the following five different zonations recognized in cathodoluminescence of carbonates: concentric, oscillatory, sectorial, mottled and homogeneous

(Reeder 1991). Zonations summarize a complexity of possible interstitial water evolution, and the diagenesis successive steps have to be identified to permit the elaboration of diagenetic sequences that can be used for establishing a lithification model (Meyers 1991). For each phase of their diagenetic sequences, the authors assume only some of these factors of luminescence.

The approach of cement stratigraphy consists of establishing the chronological order of cementation phases with the help of cement morphologies and signals of the cathodoluminescence. Diagenetic sequences can be set up on the basis of the succession of the diverse zonations encountered in carbonate cements (Machel 1985). In the case of regional cement stratigraphy, the approach also consists of observing and correlating these phases and their variations inside a reservoir rock, and then, if possible, to map on a greater scale their distributions (Meyers 1978; Barker et al. 1991; Goldstein 1991).

Image processing applied on cathodoluminescence data has been used to determine the diversity of cement types, to measure and predict porosities and cements percentages (Dorobek et al. 1987; Witkowski et al. 2000). The relative intensity of cathodoluminescence bands has also been used to classify cements and propose diagenetic sequences (Chapoulie et al. 2005). The use of digital image processing softwares, specifically developed for geological applications (Roduit 2007; Ndiaye 2008), constitutes a powerful supply for interpreting and correlating cathodoluminescence data.

2 Methods

2.1 Image acquisition

The device used for this study is a Cl8200MK5-optical cathodoluminescence with a cold cathode. We used beam conditions of 15 kV at 50–60 mA with an unfocused beam of about 1 cm. The observation chamber has a residual pressure of 80 mTorr.

Samples were non-coated. The pores to be studied were pictured as a grid from top left to bottom right in a dark room with a digital camera: with a normal grab for natural light (grab time: 3.6 s/shutter time: 55 ms), with a long time grab for cathodoluminescence (grab time: 3.6 s/shutter time: 3–5 s). The parameters were maintained fixed to avoid additional treatments. Neither filters nor standards were used for image calibration. All pictures of each pore were then assembled into images with the Photomerge tool in Photoshop CS3. This tool automatically equalizes the luminosity that tends to derive with time, and the unequal intensity due to the position of the electron beam. The final images in natural light and in cathodoluminescence have to be superimposable to facilitate the correlation between cement morphologies and cathodoluminescence signatures. These operations, assemblage, equalization and superposition, can be effectuated with the JMicrovision software developed for geological applications in Geneva University (Roduit 2007).

2.2 Image processing

The image processing methodology used in this study is based on the software recently developed for geological applications: Strati-Signal, designed for extraction, treatment and time-series analyses of stratigraphical signals (Ndiaye 2008).

This application consists of extracting signals from cathodoluminescence digital images and comparing them statistically for each diagenetic sequence through crosscorrelation. For each studied sample, the first step consists of extracting the Red channel signal from cathodoluminescence digital image, following a path perpendicular to cementation rims. This continuous signal is then converted into an ordered spectrum of maxima and minima corresponding to significant change in cementation processes (Ndiaye 2008). As the Blue channel reflects only the intrinsic cathodoluminescence of carbonates, and the Green channel is always of lower intensity levels, they were not used in the signal extraction.

The algorithm used for extracting maxima and minima is presented in Table 1. It works in two steps: the detection of all peaks and troughs based on the sense of variation of the signal, and the stacking of non-significant peaks and troughs with the closest significant peak or trough. This algorithm allows to eliminate the influence of luminescent or non-luminescent rim thickness, which makes the comparison of two signals very difficult even when they are extracted from the same pore. Noise estimation, as a ratio of the standard deviation of the CL signal, permits to significantly distinguish the extracted features as maxima and minima of the red spectrum (peaks and troughs of the CL signal) (Fig. 1). Such spectra can be then compared by crosscorrelation in order to detect similar successions of events in cements coming from different samples. The crosscorrelation allows to determine the lag at which the two data sets seem to best correlate. Well correlated data will have a high correlation coefficient at a given lag and correlation coefficient will decrease as one moves away from that lag. In the other hand, two spectra having negative or unsignificant crosscorrelation coefficients at all lags have no common diagenetic events (Ndiaye 2008). The crosscorrelation of two stationary time series X and Y can be computed using the following formula:

$$r_{XY}(k) = \frac{\sigma_{XY}(k)}{\sqrt{\sigma_X \sigma_Y}}$$

Table 1 Algorithm used for peak extraction from the cathodoluminescence image line scans

Step 1: detection of peaks and troughs
so **n**, the size of the signal to study
so **pi**, the element at the position i in the signal
so **pi−1**, the element at the position i−1 (preceding the element)
so the boolean **up** (true if the curve is ascending, otherwise false)
so the boolean **down** (true if the curve is descending, otherwise false)
Buckle: from i = 2 until i = n
{In the run i: if pi−1 < pi [up = true check in the run i−1 if down = true yes = presence of a trough]
otherwise: if pi−1 > pi [down = true check in the run i−1 if up = true yes = presence of a peak]}
Step 2: stacking of non-significant peaks and troughs
with the closest significant peak or trough
Nb: **signal2** is the result of step 1
so **s**, the standard deviation of the signal to study
so **k**, an integer number
so **r = s/k**, **r** is the threshold value (all lower variation than r is considered as being noise)
[if the variation (up or down) between two points is lower than r, the peak is considered as non-significant, r is determined by the operator after observation of the data.]
so **m**, the number of points extracted during step 1 (peaks and troughs)
so **pi**, the element at the position i in signal2
so **pi−1**, the element at the position i-1 (preceding the element i)
Buckle: from i = 1 until i = m
{If pi−1 < pi (trough case): if pi-1 <=pi + r non-significant trough, stacking with the previous trough
otherwise: if pi < pi−1 + r non-significant peak, stacking with the previous peak}

where $\sigma_{XY}(k)$ is the crosscovariance of X and Y at lag k, σ_X is the variance of X and σ_Y is the variance of Y. The crosscovariance $\sigma_{XY}(k)$ is given by the following formula:

$$\sigma_{XY}(k)\begin{cases}\frac{1}{n}\sum_{t=1}^{n-k}\left(X_t-\overline{X}\right)\left(Y_{t+k}-\overline{Y}\right) & k=0,1\ldots K\\ \frac{1}{n}\sum_{t=1-k}^{n}\left(Y_t-\overline{Y}\right)\left(X_{t+k}-\overline{X}\right) & k=-1,-2\ldots -K\end{cases}$$

where n represents the population of the shortest chronological serie, and K represents the maximum lag. In practice, these spectra have to correspond exclusively to cementation events. It is important, when positioning the extraction line, to select a path that avoids truncations and doubling-up in the signals of cementation phases (Fig. 2). Depending on the tri-dimensional pore shape, the same cement rims may reappear on extraction profiles drawn from the border to the centre of the pore. Cements being of irregular thickness and spatial repartition, it may be difficult to correlate signals from the same diagenetic sequence, and this, even at the pore size. Direct comparison of the raw signals is not easy as the varying thickness in cementation rims shifts the corresponding peaks (Fig. 2). To counteract this difficulty, the Red channel spectra (Martinez-Verdú et al. 2002) are first smoothed with a

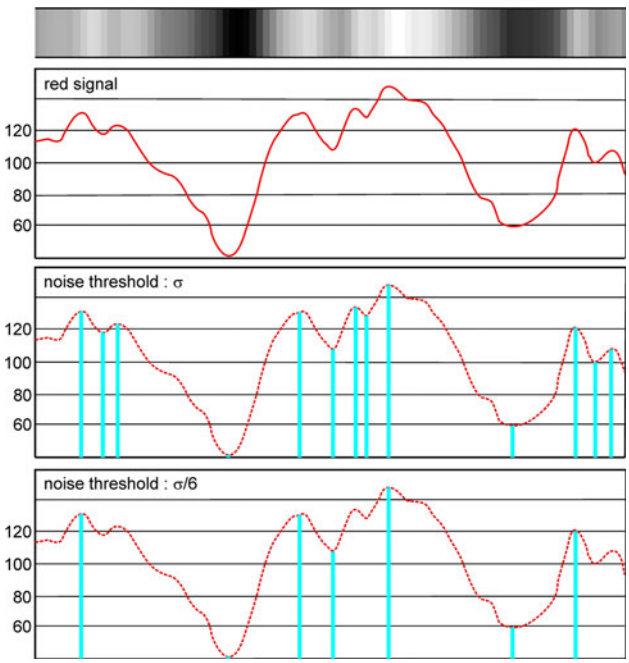

Fig. 1 Example of extraction: from the raw R signal all slope inversions are detected, minor noisy minima and maxima can be eliminated by using a threshold value based on the standard deviation of the raw signal ($r = \sigma/n$)

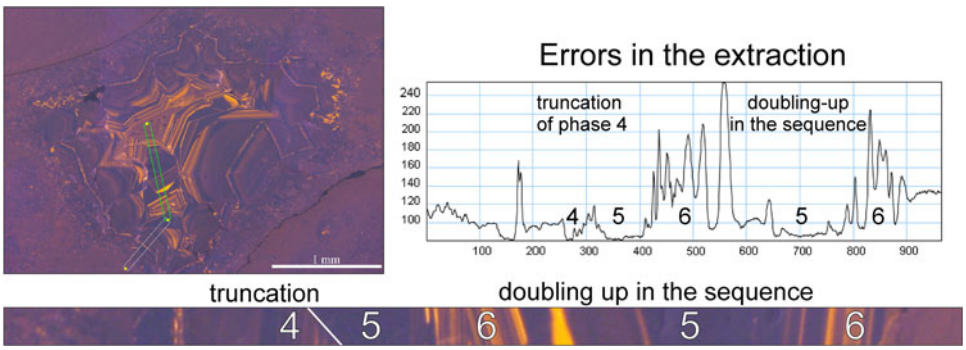

Fig. 2 Common errors in the extraction of a signal: truncation linked to geotrope structures or dissolution phases; doubling-up of the sequence linked to spatial irregularities

moving average. Then minima and maxima of the curve are extracted as peaks successions. This extraction is essential to correlate signals of different lengths. The smoothing decreases the number of extracted peaks, keeping the most significant ones. These operations are all carried out with the Strati-Signal software (Ndiaye 2008).

The visual comparison of the obtained spectra helps to correlate the cathodoluminescence signals. This comparison is made easier as the software calculates the crosscorrelation coefficient and proposes a best fit position that the user can adjust to the lag that appears to him the most significant (Fig. 7). The main incertitude comes from the difference in the number of extracted peaks, as the best fit position of crosscorrelation can be located on a set of peaks extracted from an oscillatory zonation or on a more uniform set extracted from a concentric zonation.

Crosscorrelation can be applied to complete diagenetic sequences or to selected cementation phases. The extension of cementation lens and their effective correlation remain the major difficulties of a regional study (Goldstein 1991; Meyers 1991).

2.3 Petrographic and geochemical analyses

Cathodoluminescence being a non-destructive method, the same thin sections were used for further petrological and geochemical analyses. Mapping of trace elements was performed on an EAGLE III XPL EDAX X-microfluorescence device. It is a semi-quantitative non-destructive method that does not require any sample preparation. Samples are positioned in the chamber, put under vacuum and the area to be mapped is defined, in this case a cemented pore of a thin section. Mapping was performed for Fe and Mn, which minimum detection limits are around 20–30 ppm for dry samples, limits that are still relevant for a cathodoluminescence response to Fe^{2+} and Mn^{2+} contents.

The same thin sections were finally studied with alizarin red S and potassium ferricyanide staining by petrological microscopy. This coloration permits the differentiation of calcite from dolomite, and Fe-bearing from Fe-free calcite and dolomite. These results allow direct comparison of Fe-bearing calcite and dolomitic areas with the cathodoluminescence intensity.

Microthermometry of fluid inclusions was performed with a LINKAM 600 device and digital camera assembled on a microscope. The difficulties with calcite cements reside in the preservation of primary inclusions after neomorphism, in avoiding the reequilibrated inclusions due to microcracks and necking-down, and in distinguishing clearly the bubble behavior with the crystal lattice birefringence. Therefore, most inclusions were measured in blocky spar cements. Temperatures of homogenization were measured first and temperatures of melting ice in second, as the fluid inclusions are indeed often dilated, or cracked, by the volume increase of the water freezing. The homogenization temperatures help modeling the *P*/*T* conditions of fluid entrapment, the melting ice temperatures can be converted to equivalent NaCl percentages, or fluid salinity.

3 Case study

3.1 Location and stratigraphic settings

Two sections were analysed and sampled in the Mount Salève (Haute-Savoie, France), at the base of the Tidalites de Vouglans Formation in the Grande Oolithe Member (Charollais and Badoux 1990). The two outcrops are situated in the surroundings of the Etiollets esplanade (Fig. 3). In this case study, only two significant samples are considered (Fig. 4).

The Grande Oolithe Member is composed of oolithic and bioclastic shoals containing numerous oncoids. The depositional environment shifts from back-reef to external lagoon and regresses to lacustrine environment, presaging the Purbeckian facies. The Tidalites de Vouglans are considered as a shallowing-upward sequence (Strasser et al. 1999) and show frequent facies lateral variations. When algal mats are not present, rocks are usually devoided of organic matter. The two samples were selected at

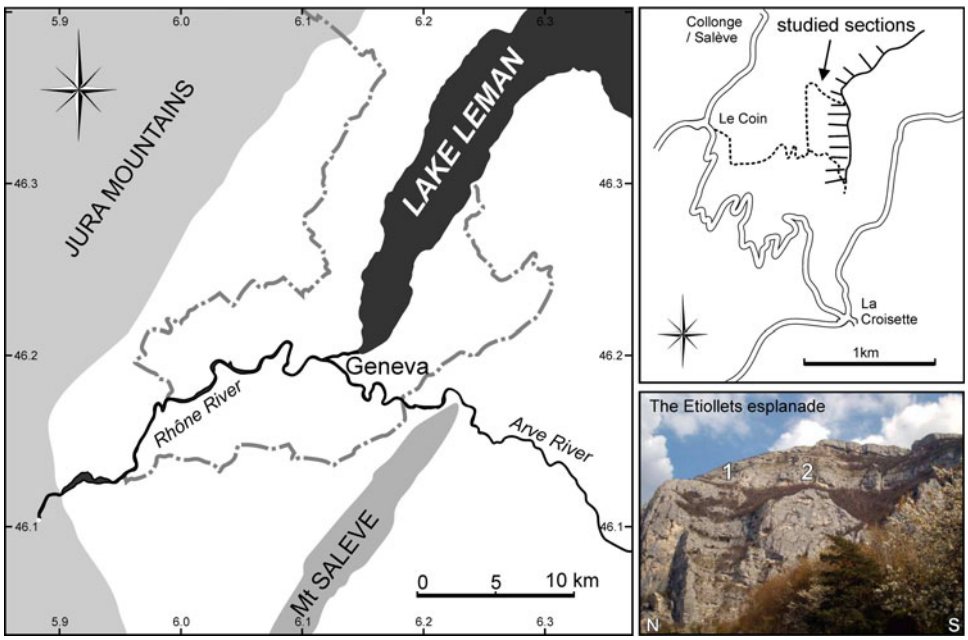

Fig. 3 Location of the case study in the Mount Salève (46.1°N/6.1°E). The two outcrops are part of the Kimmeridgian formation of the Tidalites de Vouglans (Grande Oolithe Member)

the base of the Grande Oolithe where pores are larger and where they can show more complete and regular cementation sequences.

Regarding the Salève period to present time, sedimentation stops on the platform during the Barremian. Its stratigraphy ends with the Urgonian limestone. At the end of the Cretaceous, the first alpine compression provokes the emersion, fracturation and tilting of the platform. The Cretaceous limestones are exposed to weathering and undergo an important karstification. At the end of the Tertiary, the Mount Salève undergoes paroxystic tectonic thrusts which give it its actual shape with the frontal reversed serie and the Coin thrust fault (Charollais and Badoux 1990). Regarding the Salève stratigraphy, the Hauterive marls and the Siderolithic can act as sources of iron and manganese in circulating fluids.

3.2 Diagenetic sequences

The morphologies of cements observed in natural light reveal phreatic and vadose diagenetic environment (Fig. 5a, b; Chafetz et al. 1985; Harris et al. 1985).

Figures 5e and f show the delimitations of the cementation phases visible on cathodoluminescence and the positions of the scan lines. Eight stages of diagenetic processes were recognized in the evolution of the Grande Oolithe Member: cementation, neomorphism, compaction, cementation, dissolution, fracturation, cementation and dolomitization. Fracturation is added with two generations of calcite veins (Fig. 5g). Figures 5c and d assess that the linescans do not intersect with meteoric dolomite areas that could have shifted the luminescence signal to red or brown.

Looking at the natural light and cathodoluminescence images of sample A (Fig. 5a, e), phases 1 and 2 correspond to an equigranular cement with a dogtooth cement overgrowth in dull orange mottled zonation and are relics of early marine cements. Figures 5c and 6 show Fe-bearing calcite and detectable traces of incorporated iron in the pore cement rims, causing the dull luminescence. For instance, microbes are common agents of micritization and early cementation (Neumeier 1998). They can also trigger the incorporation of iron, as their metabolism consumes rapidly the oxygen at disposal in the pore space. However, the lack of organic matter argues against a sustainable anaerobic activity. An early marine stage is thus inferred. The scalenohedral cement of the phase 3 of sample A is also a cement related to an early diagenesis (Purser 1983). These scalenohedrons are clearly visible in blue on the coloration images, although partially dissolved on sample B (Fig. 5c, d). This type is formed in various phreatic environments, but its dull brownish to dull orange concentric zonation ending with an extinct band argues for a marine environment. It is followed by an orange luminescent rim. Again, Figs. 5c and 6 show the influence of iron incorporation as a cause of dull luminescence. The luminescent rim is interpreted as a pause in the cementation process as, not being actually oscillatory, it cannot infer for reequilibration of pore fluid or increase of growth rate. It can be partially linked to a more proximal facies, such as the lacustrine facies described on Fig. 4. These three phases are reported on Fig. 5e as sequence 1. Mechanical compaction occurs after the development of phases 1–3 as demonstrated by their detachment from the surface of the grains (Fig. 5h). Compaction leads to porosity reduction.

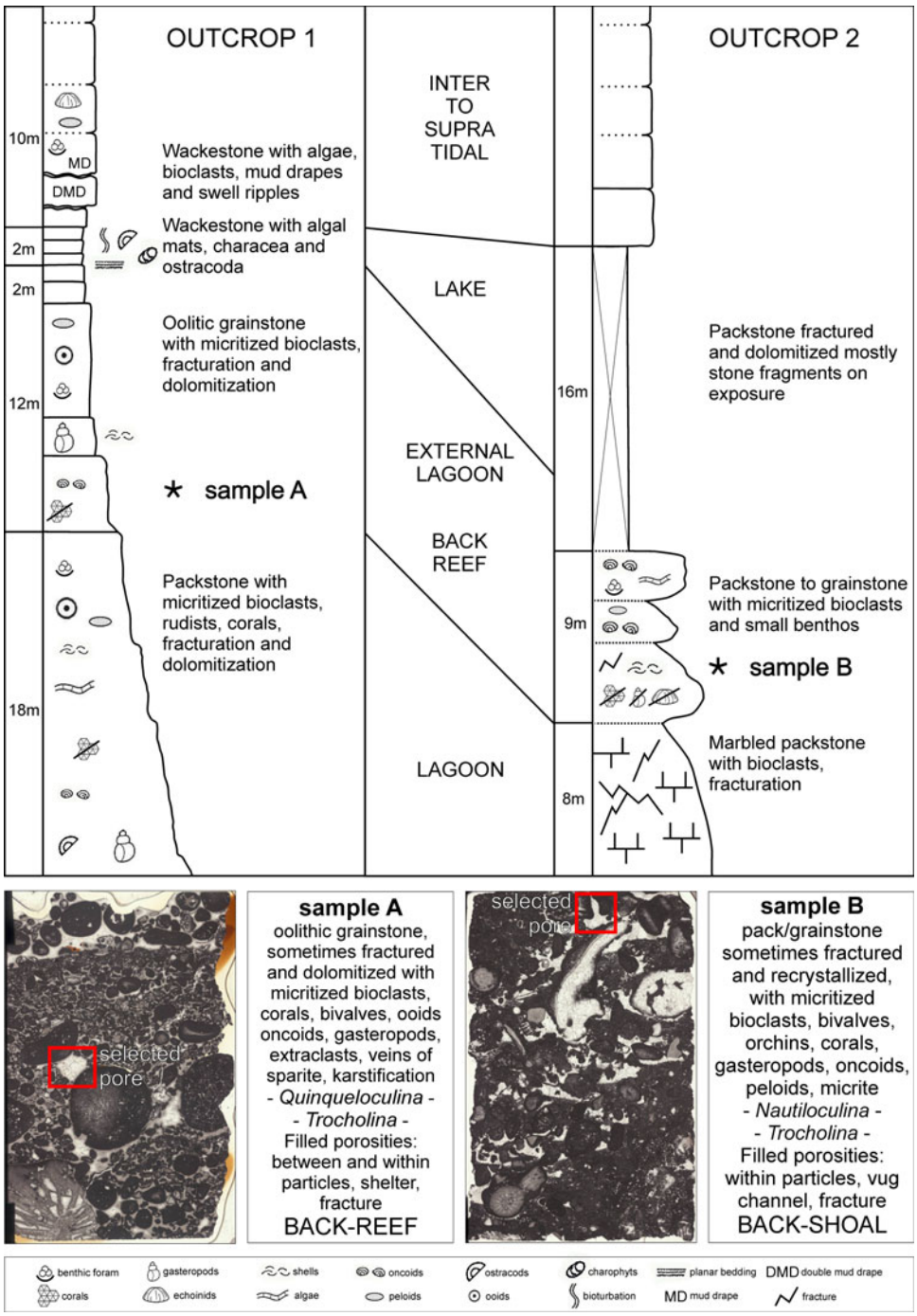

Fig. 4 Synthetic logs of the two outcrops with short petrographic descriptions and correlation of depositional environments. Note the position of the samples A and B. *Pictures* of the *thin* sections of samples A and B with description. The selected pores are *squared* in *red*

Expelled fluids turn to autochthonous cementation which luminescence is identical to the surrounding. Such a cementation linked to autochthonous fluids is visible in sample B (phase 1, Fig. 5f), in this case very dull brownish, which its more micritic facies has kept less permeable.

Sample B shows remnants of the scalenohedral cement (Fig. 5d, f), with partially dissolved scalenohedrons and meteoric micro-dolomite inclusions superimposed (Harris et al. 1985; Warren 2000). This phase is not taken into account in sample B diagenetic sequence as the vadose environment, testified by a stalagmitic cement (Fig. 5b), favoured neomorphism and dissolution of early phases. Oscillations between phreatic and vadose environments in early diagenesis can be explained by the coastal variations of the Tidalites de Vouglans associated with the regressive tendency of the Pürbeckian. Alternate wetting and drying of coarse sediments can be the cause of asymmetric cementation (Purser 1969; Fig. 5b). Microstalagmitic cements have been reported as early vadose phases in

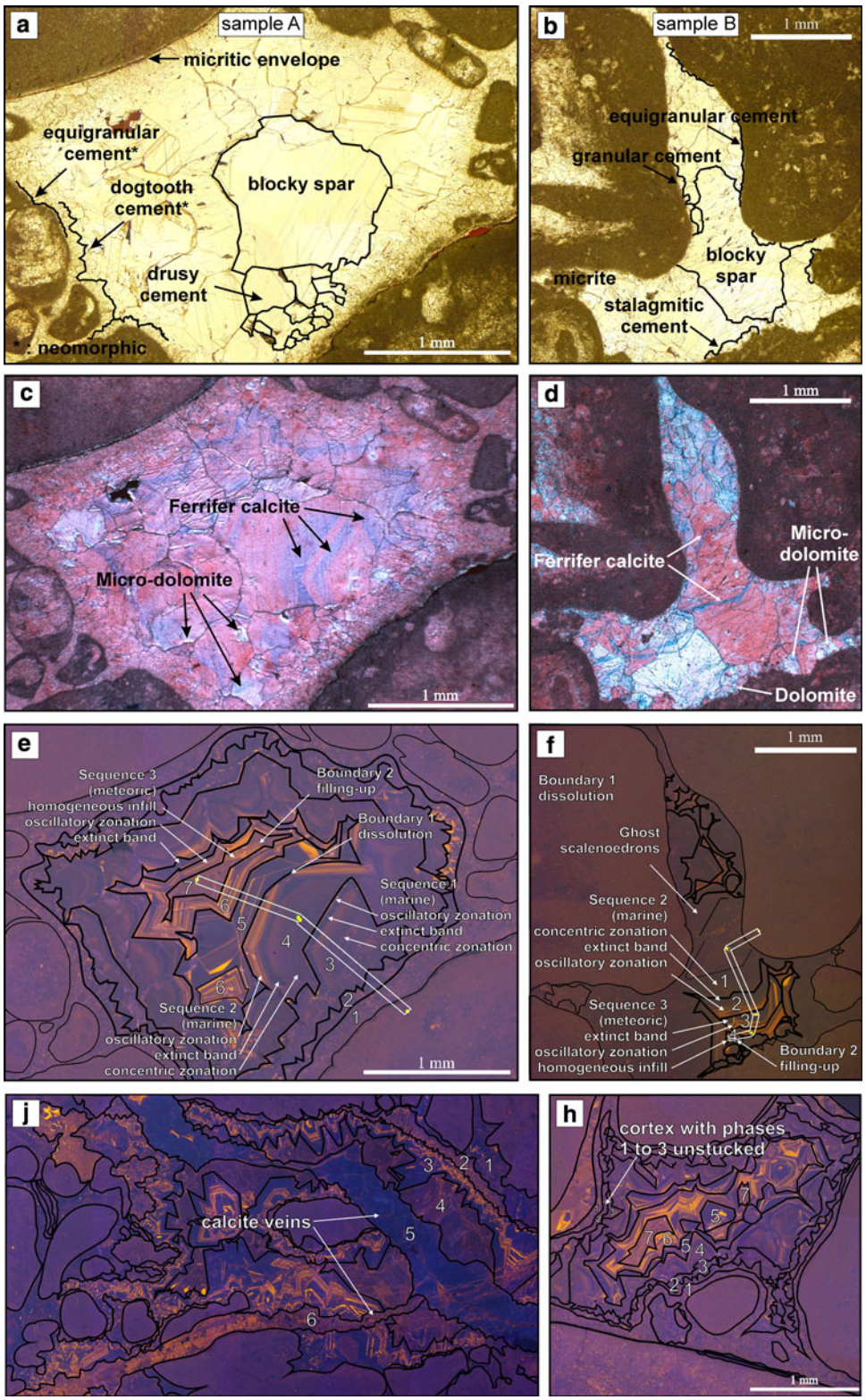

Fig. 5 Selected pores of samples A and B. **a**, **b** Pores in natural light with cement morphologies overlined. **c**, **d** Pores *colored* with alizarin S red and potassium ferricyanure, with dolomite, micro-dolomite and ferrifer calcite *overlined*. *Colors* significances: *red* calcite, *white* dolomite, *blue* ferrifer calcite. **e**, **f** Pores in cathodoluminescence with cementation phases *overlined*. *Lines* of signal extraction are also shown. **g**, **h** Diagenetic events, fracturation and compaction, illustrated by two cathodoluminescence pictures from samples of outcrop 1

beachrocks (Hanai and Oji 1981), and oolites (Searl 1989; Müller 1971). Thus, the phase in sample B is here interpreted as an early cement, but, facing an important superimposed meteoric stage, cement morphologies interpretations should be taken with caution, as the same argument of alternate wetting and drying can be applied later to karstified and fractured types of aquifer.

Phase 4 of sample A and phase 1 of sample B are considered as synchronous cements. These phases are located within the blocky spar cements (Fig. 5a, b). Both

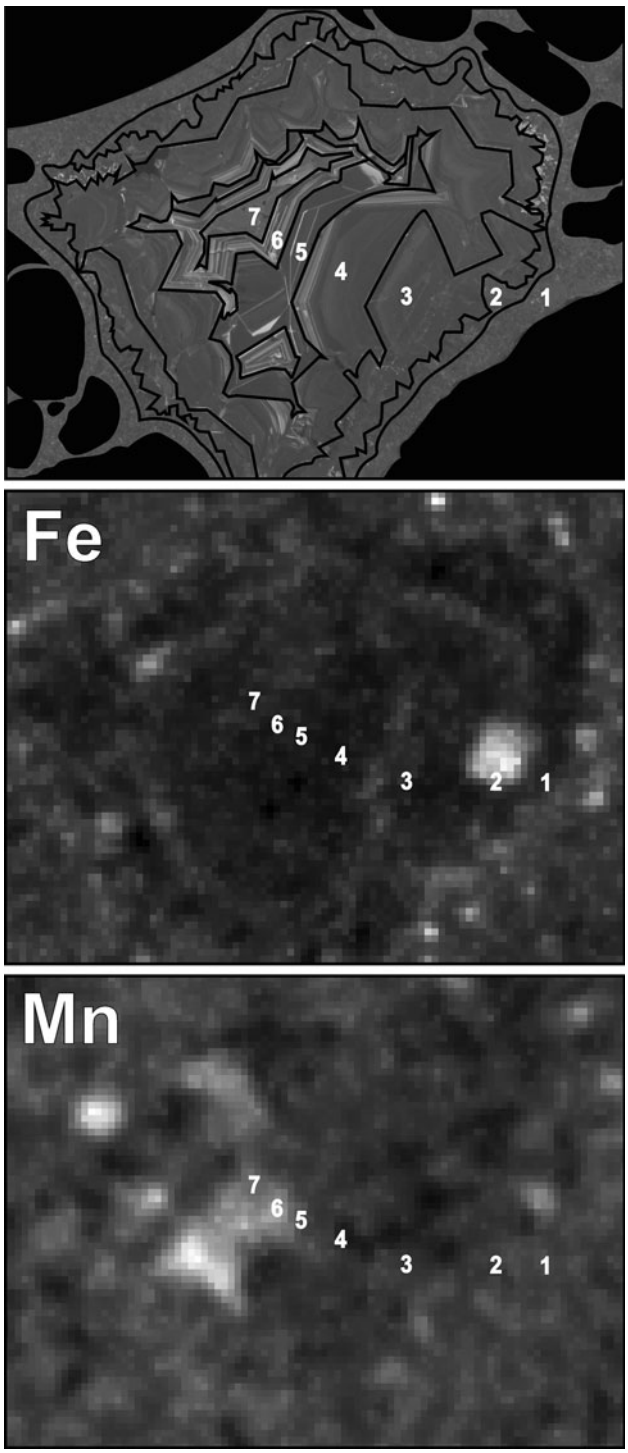

Fig. 6 X-microfluorescence mapping on sample A: results for Fe and Mn. The diagenetic phases are reported on Fe and Mn maps to better correlate trace element contents with the cement luminescence intensity

show a concentric zonation of weak orange luminescence followed by an extinct stripe and a bright orange oscillatory zonation. These two phases are truncated by a dissolution phase. The phases 4 and 1 are reported on Figs. 5e and f as sequence 2 and boundary 1. Figure 5c shows that the iron content is decreasing from the beginning to the end of this cementation phase. It is then followed by the oscillatory zonation that can be explained by a quick chemical re-equilibration of the pore fluid. However, their origin remains uncertain. The dissolution phase argues for a change in Ca^{2+} activity and sudden sub-saturation of pore fluid. Figure 5g shows two different fracture infills, one extinct and one luminescent, and Table 2 shows two different ranges of salinity in the observed fluid inclusions. The measured melting ice temperatures argue for meteoric fluids circulating in fractures while the measured homogenization temperatures indicate various *P*/*T* conditions mainly related to either faults were active or not (Schegg and Moritz 1993). The calcite vein lacking luminescecnce is associated with inclusions of low salinity range, and is considered as the most credible source for fluids dissolving phase 4 of sample A and phase 1 of sample B. Freshwaters circulating in aquifers are exposed to very local variations modifying trace elements concentration ratios and Ca^{2+} activity (Machel and Burton 1991; Machel 1999). This dissolution can be related to prior karstification or later fracturation. However, making a correspondence between geological events and cement chronology remains hazardous. Dolomitization is considered as a continuous meteoric process of Mg^{2+} displacement from magnesian calcite to dolomite happening in a closed-like system (Harris et al. 1985; Warren 2000).

Phases 5–7 and 3–4 of samples A and B, respectively, displayed on Fig. 5e and f as sequence 3, show an extinct stripe of cement following this dissolution phase, then a bright orange to yellow oscillatory zonation and a final homogeneous orange luminescent infill (Fig. 5e, f: boundary 2). Figure 6 shows that Mn detection is maximal at the centre of the pore and can be considered as the cause of the final infill cement luminescence. Sequence 3 was also associated with the luminescent calcite vein, actually cutting the previous vein (Fig. 5g), and with the inclusions of around 2% NaCl eq. salinity (Table 2), assessing its higher Mn^{2+} activity (Fig. 6).

This negative sequence (Amieux 1982) is interpreted as meteoric cementation lenses that flowed through the fracturation network under various pressures, becoming less oxic during its progression in the rock. This statement is assessed by the meteoric dolomitization (Fig. 5c, d), by the calcite veins associated with fluid inclusions of low salinities, and also by the nonferroan nature of these cements (Figs. 5c, d, 6). Indeed, cements of deep burial diagenesis show in general positive sequences, evolving to a dull luminescence (Grover and Read 1983). The Mount Salève tectonic history also rejects the possibility of burial diagenesis.

Table 2 Results of fluid inclusions microthermometry for samples from outcrops 1 and 2, with temperatures of homogenization (T° h.), temperatures of melting ice (T° m. ice) and salinity calculated as equivalent percentages of halite (% eq. NaCl)

Inclusions	T° (h.)	T° (m. ice)	% equiv. NaCl
Outcrop 1			
1	83.9	0	0
2	86.6	−0.3	0.5
3	86.5	−0.3	0.5
4	88.8	−0.3	0.5
5	85.3	−0.7	1.2
6	84.2	−0.8	1.4
7	83.9	−1.1	1.9
8	76.7	−1.1	1.9
9	73.5	−1.2	2.1
Outcrop 2			
1	77.3	−0.4	0.7
2	86.7	−0.5	0.9
3	82.8	−0.5	0.9
4	73.5	−0.5	0.9
5	82.3	−0.5	0.9
6	80.2	−0.5	0.9
7	86.8	−0.6	1.1
8	76.4	−0.6	1.1
9	72.4	−0.6	1.1
10	81.5	−0.7	1.2
11	93.7	−1.2	2.1
12	92.5	−1.2	2.1

3.3 Signal extraction

Image processing is used for obtaining digital signals specific of the zonations of each cementation phase. The extraction is executed on Strati-Signal. On the extraction line of sample A (Fig. 7), three to four zones can be distinguished: the concentric zonation which records a progressive change in the fluid, the oscillatory zonation indicating fast precipitation from an oversaturated fluid (Reeder 1991), the mottled zonation due to neomorphism and a final luminescent homogeneous infill. Two luminescence-free zones are also identifiable. Those zones are assumed to be suites of meteoric fluids of low trace elements activities. A short sequence attributable to diagenetic processes is established this way.

The extraction line of sample B shows obviously zonations that corroborate partially the extraction sequence of sample A. The final successions of both samples are similar: concentric zonation, oscillatory zonation, extinction, oscillatory zonation, final luminescent homogeneous infill. After smoothing the R signals by moving average, 57 extrema are extracted from the sequence of sample A and 41 from the sequence of sample B.

3.4 Correlation of samples A and B

The diagenetic sequence of sample A is composed of seven steps. The diagenetic sequence of sample B is composed of four steps and shows a somehow duller luminescence, linkable to autochthonous cementation and further important meteoric diagenesis. However, the succession of zonations in cathodoluminescence appears similar for both extraction lines: concentric, oscillatory, extinction, oscillatory and homogeneous infill (Fig. 7).

The aim is now to correlate these diagenetic sequences or cementation phases by using image processing of extracted spectra, knowing that these sequences show variable numbers of peaks and variable luminescence intensities and that the first phases of sample A look specific. The unequal lengths of signals and the thickness variability at the luminescent zones make also the visual correlation difficult.

The crosscorrelation (Fig. 7) of the two extrema sequences shows that the best fit is obtained for a positive lag of 6 with a crosscorrelation coefficient reaching 0.78. The superimposition of the two sequences reveals a good similarity and indicates that the pore fluids followed similar conditions of evolution (Reeder 1991; Pagel et al. 2000). They belong thus to the same cementation lense (Plunkett 1997).

4 Discussion

As the diagenetic sequences are punctual recordings of regional processes, the extracted luminescence signal has to overlay the major part of the diagenetic events in order to be treated statistically. Every extraction line should contain the general diagenetic chronology. This implies a preliminary study of the regional geology with petrographic and geochemical analyses of the rock samples. As in the present case study, coastal shorelines are deposition environments of high variability with changes in permeability and porosity to which early to late diagenesis add even more variability to the primary conditions. Concerning the cathodoluminescence, similar zonations can be found in very different diagenetic environment. For example, oscillatory zoning can be obtained as well in the mixing zone as in the deep burial environment (Meyers 1991). The user being aware of the limiting factors, such as dissolution, missing events or superimposition of meteoric dolomite, basic information should first be gathered through detailed petrographic analyses. Then, facing many interpretations (Machel and Burton 1991), it should be kept in mind that this methodology, even if statistical, remains qualitative and was developed to facilitate the correlation of cementation events from the same diagenetic environment. The studied outcrops were at 500 m distance

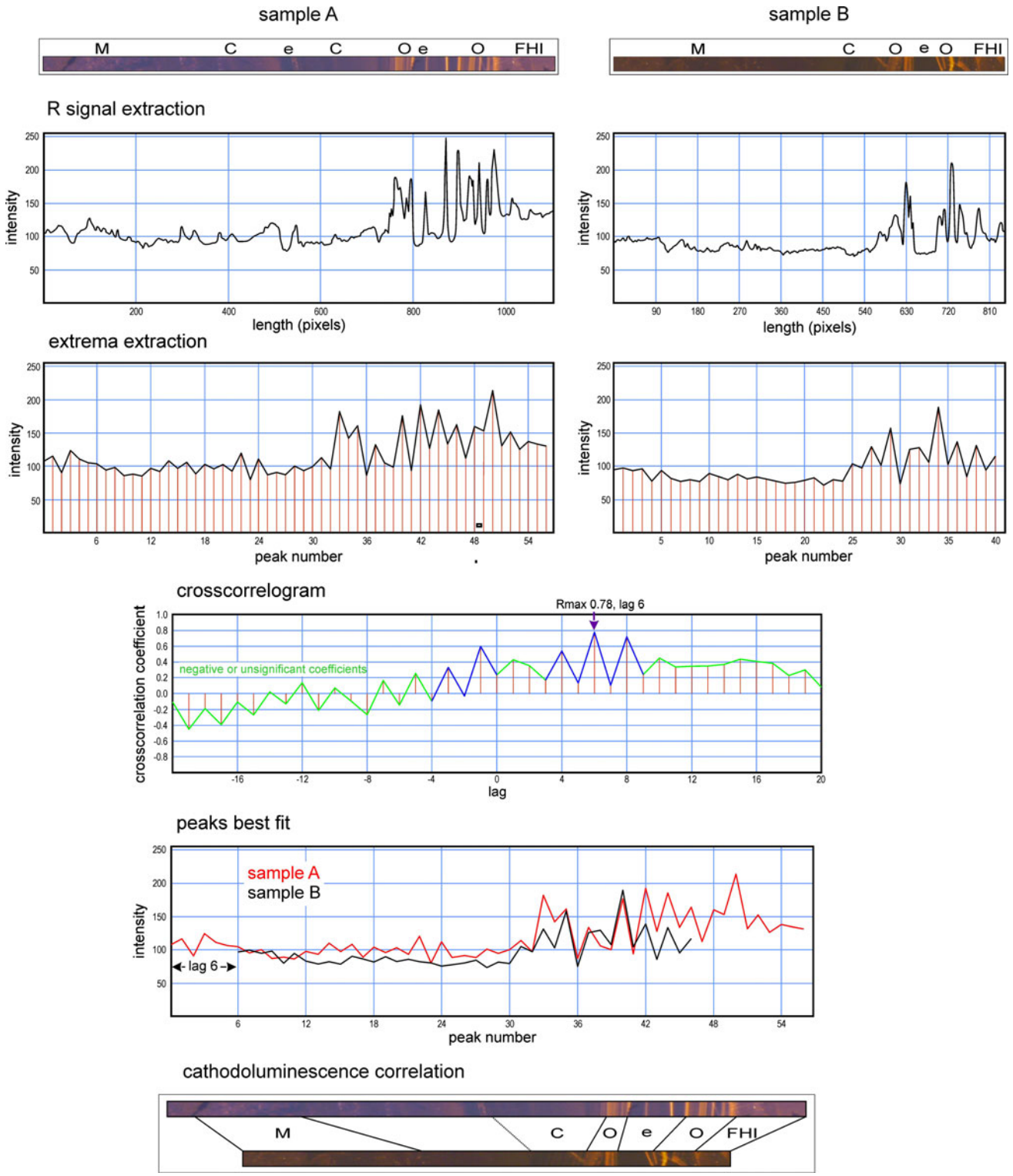

Fig. 7 Crosscorrelation of the two cement sequences. From *up* to *down* cement sequences (*M* mottled, *C* concentric, *e* extinct, *O* oscillatory, *FHI* final homogeneous infill); extracted R signal profiles; extracted peaks from the R profiles after smoothing by moving average; crosscorrelogram of A and B sample *peaks*. On the basis of a Student test, significant lags are *overlined* in *blue* and unsignificant lags in *green*; best fit position of the superposed of A and B sample *peaks*; features correlation of the cathodoluminescence zonations for the two extracted *lines*

to each other. Although sample A has three cementation steps not in common with sample B, thus inducing a lag of 6 when overlaying their respective peaks, their crosscorrelation index still reaches 0.78. Cases of porosity infill by early autochthonous cementation were also encountered, but not considered to be relevant.

5 Conclusions

Cement stratigraphy is a powerful tool for deciphering the diagenetic history of reservoir rocks. However, the visual study and comparison of cathodoluminescence images is difficult and often unreliable. The use of digital methodology offers a more rigorous quantitative approach. The comparison of cement stratigraphy records is greatly facilitated by the extraction of digital signals, as long as they follow the growth direction of the cement. It permits to obtain a raw sequence that can be compared to any other signal by crosscorrelation. The use of luminescence extrema rather than the raw signal permits to get rid of the thickness variations of the cementation phases. Extrema can be found using the Strati-Signal software (Ndiaye 2008), which provides a way of testing statistically the similarity of cements, a high crosscorrelation coefficient being proof of same diagenetic events. The authors admit that standard petrological analyses and field selections have to be lead preliminarily in order to interpret and benefit from the method correlation results, such as the lag positioning or the number of extracted peaks. Once the main diagenetic sequence is well-defined, it can provide the base of interpretation for more distal samples. The use of the method proposed in this paper helps to reconstruct the diagenetic history of reservoir rocks even when the diagenetic signal recorded in cements is highly variable or truncated by local dissolution phases. As regional cement stratigraphy is normally applied to reservoir studies, the authors admit that case studies different from field equivalents would advantageously complement their demonstration with examples affected by the deep burial diagenesis.

Acknowledgments Special thanks to Nicolas Roduit for his advices on image processing, and to Edwin Gnos for his constructive remarks. This work is partially supported by the Swiss National Science Foundation (R. Martini grant # 200021-130238). JMicrovison and Strati-signal can be found on open access on the internet. The corresponding theses are also available as cyberdocuments on the following links: http://www.unige.ch/cyberdocuments/theses2007/RoduitN/meta.html, http://www.unige.ch/cyberdocuments/theses2007/NdiayeM/meta.html.

References

Amieux, P. (1982). La cathodoluminescence: méthode d'étude sédimentologique des carbonates. *Bulletin des Centres de Recherches Exploration-Production Elf Aquitaine, 6*, 437–483.

Barker, C. E., Higley, D. K., & Dalziel, M. C. (1991). Using cathodoluminescence to map regionally zoned carbonate cements occurring in diagenetic aureoles above oil reservoirs: initial results from the Velma oil field, Oklahoma. In: C. E. Barker and O. C. Kopp (Eds.), *Luminescence Microscopy: Quantitative and Qualitative Aspects* (pp. 155–160). SEPM Short Course, 25.

Cazenave, S., Duttine, M., Villeneuve, G., Chapoulie, R., & Bechtel, F. (2003). Cathodoluminescence orange (620 nm) de la calcite. I. Rôle du manganèse et du fer. *Annales de Chimie—Science des Matériaux, 28*, 135–147.

Chafetz, H. S., Wilkinson, B. H., & Love, K. M. (1985). Morphology and composition of non-marine carbonate cements in near-surface settings. In: N. Schneidermann & P. M. Harris (Eds.), *Carbonate Cements* (pp. 337–347). SEPM Short Course, 36.

Chapoulie, R., Cazenave, S., & Cerepi, A. (2005). Apport de la cathodoluminescence à haute résolution à l'étude de la diagenèse météorique dans les formations sédimentaires carbonatées. *Comptes Rendus Géoscience, 337*, 337–346.

Charollais, J., & Badoux, H. (1990). *Guides géologiques régionaux: Suisse lémanique, pays de Genève et Chablais* (p. 224). Paris: Masson.

Dorobek, S. L., Read, J. F., Niemann, J. M., Pong, T. C., & Haralick, R. M. (1987). Image analysis of cathodoluminescent-zoned calcite cements. *Journal of Sedimentary Petrology, 57*, 766–770.

Goldstein, R. H. (1991). Practical aspects of cement stratigraphy with illustrations from Pennsylvanian limestone and sandstone, New Mexico and Kansas. In: C. E. Barker & O. C. Kopp (Eds.), *Luminescence microscopy: quantitative and qualitative aspects* (pp. 123–131). SEPM Short Course, 25.

Grover, G., Jr., & Read, J. F. (1983). Paleoaquifer and deep burial related cements defined by regional cathodoluminescent patterns, middle Ordovician carbonates, Virginia. *The American Association of Petroleum Geologists Bulletin, 67*, 1275–1303.

Hanai, T., & Oji, T. (1981). Early Cretaceous beachrocks from the Miyako group, Northeast Japan. *Proceedings of the Japan Academy, Series B, 57*, 362–367.

Harris, P. M., Kendall, C. G. St. C., & Lerche, I. (1985). Carbonate cementation—a brief review. In: N. Schneidermann & P. M. Harris (Eds.), *Carbonate Cements*. (pp. 79–95) SEPM Short Course, 36.

Machel, H. G. (1985). Cathodoluminescence in calcite and dolomite and its chemical interpretation. *Geoscience (Canada), 12*, 139–147.

Machel, H. G. (1999). Effects of groundwater flow on mineral diagenesis, with emphasis on carbonate aquifers. *Hydrogeology Journal, 7*, 94–107.

Machel, H. G., & Burton, E. A. (1991). Factors governing cathodoluminescence in calcite and dolomite, and their implications for studies of carbonate diagenesis. In: C. E. Barker & O. C. Kopp (Eds.), *Luminescence microscopy: quantitative and qualitative aspects* (pp. 37–57). SEPM Short Course, 25.

Martinez-Verdú, F., Pujol, J., & Capilla, P. (2002). Calculation of the color matching functions of digital cameras from their complete spectral sensitivities. *Journal of Imaging Science and Technology, 46*, 15–58.

Meyers, W. J. (1978). Carbonate cements: their regional distribution and interpretation in Mississippian limestones of southwestern New Mexico. *Sedimentology, 25*, 371–400.

Meyers, W. J. (1991). Calcite cement stratigraphy: an overview. In: C. E. Barker & O. C. Kopp (Eds.), *Luminescence microscopy: quantitative and qualitative aspects* (pp. 133–148). SEPM Short Course, 25.

Müller, G. (1971). "Gravitational" cement: An indicator for the vadose zone of the subaerial diagenetic environment. In: O. P. Brücker (Ed.), *Carbonate cements* (pp. 301–302). Studies in Geology, 19.

Ndiaye, M. (2008). A multipurpose software for stratigraphic signal analysis. PhD thesis 3930, Section des Sciences de la Terre, Université de Genève, 118 pp.

Neumeier, U. (1998). Le rôle de l'activité microbienne dans la cimentation précoce des beachrocks (sédiments intertidaux). PhD thesis 2994, Section des Sciences de la Terre, Université de Genève, 183 pp.

Pagel, M., Barbin, V., Blanc, P., & Ohnenstetter, D. (2000). *Cathodoluminescence in geosciences* (p. 514). Heidelberg: Springer.

Plunkett, J. M. (1997). Early diagenesis of shallow platform carbonates in the Oxfordian of the Swiss Jura Mountains. PhD thesis 1158, Institut de géologie de Fribourg (Suisse), 167 pp.

Purser, B. H. (1969). Syn-sedimentary marine lithification of Middle Jurassic limestones in the Paris Basin. *Sedimentology, 12*, 205–230.

Purser, B. H. (1983). Sédimentation et diagenèse des carbonates néritiques récents. Tomes 1 et 2. Cours de l'école nationale supérieure du pétrole et des moteurs. Editions Technip, Paris.

Reeder, R. J. (1991). An overview of zoning in carbonate minerals. In: C. E. Barker & O. C. Kopp (Eds.), *Luminescence microscopy: quantitative and qualitative aspects* (pp. 77–82). SEPM Short Course, 25.

Richter, D. K., Gotte, T., Gotze, J., & Neuser, R. D. (2003). Progress in application of cathodoluminescence (CL) in sedimentary petrology. *Mineralogy and Petrology, 79*, 127–166.

Roduit, N. (2007). JMicroVision : un logiciel d'analyse d'images pétrographiques polyvalent. PhD-thesis 3830, Section des Sciences de la Terre, Université de Genève. Program: http://www.jmicrovision.com/.

Schegg, R., & Moritz, R. (1993). Indications of paleogeothermal anomalies in the Molasse basin (Switzerland and France). Geofluids'93 extended abstracts, 96–99.

Searl, A. (1989). Diagenesis of the Gully Oolite (Lower Carboniferous), South Wales. *Geological Journal, 24*, 275–293.

Strasser, A., Pittet, B., Hillgartner, H., & Pasquier, J.-B. (1999). Depositional sequences in shallow carbonate-dominated sedimentary systems: concepts for a high-resolution analysis. *Sedimentary Geology, 128*, 201–221.

Warren, J. (2000). Dolomite: occurrence, evolution and economically important associations. *Earth-Science Reviews, 52*, 1–81.

Witkowski, F. W., Blundell, D. J., Gutteridge, P., Horbury, A. D., Oxtoby, N. H., & Qing, H. (2000). Video cathodoluminescence microscopy of diagenetic cements and its applications. *Marine and Petroleum Geology, 17*, 1085–1093.